Article | Received 11 June 2026; Revised 20 July 2026; Accepted 23 July 2026; Published 18 August 2026
https://doi.org/10.55092/asymmetry20260005

Matching of perturbative and exponentiated initial state radiation corrections to e^+e^--annihilation

Andrej Arbuzov[1,2,*] and Uliana Voznaya[1,2]

[1] Bogoliubov Laboratory for Theoretical Physics, Joint Institute for Nuclear Research, Dubna, Russian Federation
[2] Institute of Engineering and Physics, Dubna State University, Dubna, Russian Federation

* Correspondence author; E-mail: arbuzov@theor.jinr.ru.

Highlights:

- An advanced scheme to match perturbative results on higher-order radiative corrections with exponentiated contributions is suggested.
- A modified scheme for simultaneous exponentiation of photonic and pair corrections is proposed.
- The results are relevant for future e^+e^- colliders including FCC-ee and CEPC.
- A new subtraction scheme instead of the $\overline{\text{MS}}$ is suggested.

Abstract: The behavior of higher-order radiative corrections due to initial state radiation in processes of electron-positron annihilation is analyzed. Numerical results for energies of future colliders are presented. Uncertainties of the known results on these corrections are estimated. A modified scheme for simultaneous exponentiation of pure photonic and non-singlet pair corrections is presented. Matching of the exponentiated results with the existing analytic higher-order calculations is constructed. A new subtraction scheme is suggested. The results obtained are important for increasing the relative accuracy of the theoretical description of processes that will be studied in future electron-positron colliders to a level of approximately 10^{-5}.

Keywords: radiative corrections; exponentiation; parton distribution functions; QED; electron-positron annihilation

1. Introduction

Precise theoretical predictions of radiative corrections to electron-positron annihilation are important for experiments at future electron-positron colliders like FCC-ee [1] and CEPC [2]. Despite the great progress in the development of multi-loop calculation methods, computing higher-order radiative corrections to realistic differential observables in high-energy physics remains a complex task. Meanwhile, the accuracy of the analysis of many observables, first of all related to precision tests of the Standard Model and extraction of its parameters, suffers from uncertainties in the theoretical description of effects due to initial state radiation [3]. One of the methods that allows evaluation of higher-order corrections without their direct calculations is exponentiation of known lowest-order results, which performes a reorganization of the perturbative expansion and resummation of certain contributions to all orders. Another powerful method is the so-called QED structure function approach [4], which allows one to calculate systematically the part of higher-order corrections enhanced by powers of large logarithms. In this article, we discuss matching of these approaches and estimate the corresponding theoretical uncertainties.

Exponentiation in particle physics has been studied since 1960s. In the work of D.R. Yennie, S.C. Frautschi, and H. Suura [5] infrared divergences were resummed into a universal exponential factor. In the Yennie-Frautschi-Suura (YFS) exponentiation formalism, all photons emitted in processes like electron scattering by a potential, bremsstrahlung off nucleons, *etc.*, are separated into soft and hard parts based on their energy, and radiation of soft and virtual photons is associated with infrared singularities, which cancel each other. The remaining contribution can be re-summed in an exponential form. There are also some Monte-Carlo (MC) simulation programs based on the YFS method: PHOTOS [6], KKMC [7], BHLUMI [8,9], Sherpa [10], and others. Exponentiation of the pure photonic part of the electron structure function (parton distribution function) was derived by V.N. Gribov and L.N. Lipatov [11]. E.A. Kuraev and V.S. Fadin [4] suggested an ad hoc exponentiation procedure which allows to improve accuracy of the finite order perturbative solution and to take into account a part of pair corrections. In the work by G. Passarino [12], connection between exponentiation and structure functions is discussed in detail. Amplitude-based resummation in collinear and infrared (IR) limits and its YFS MC realization was discussed in the work [13], and Coherent Exclusive Exponentiation (CEEX) [14] and Exclusive Exponentiation (EEX) [15] realization was discussed in [16].

The method of structure functions was introduced first for QED in the work of V.N. Gribov and L.N. Lipatov [17], where the electron structure functions were obtained. The Dokshitzer–Gribov–Lipatov–Altarelli–Parisi evolution equations [18,19] were derived for QCD based on the latter approach, and they were reduced back to the QED case by E.A. Kuraev and V.S. Fadin [4]. There are numerous applications and further developments of the method within the leading logarithmic approximation, see e.g. references [20–23]. Application of the method in the next-to-leading order (NLO) approximation was demonstrated for the first time in [24] for derivation of QED radiative corrections due to initial state radiation (ISR) in electron-positron annihilation. Then it was applied for calculations of $\mathcal{O}(\alpha^2 L)$ corrections to a few other processes including muon decay, deep inelastic scattering [25], Bhabha scattering, and charge and helicity asymmetries. The structure function approach allows avoiding direct loop calculations. But only the most numerically significant corrections are taken into account. These are corrections enhanced by the so-called large logarithm

$$L = \ln \frac{\mu_F^2}{\mu_R^2}, \tag{1}$$

where μ_F is factorization scale and μ_R is renormalization scale. The natural choice of μ_R in QED is the electron mass, and μ_F should correspond to a characteristic (high) energy of the process.

An alternative approach is the soft-collinear effective theory (SCET) which allows to separate soft and hard collinear contributions in an easier way [26–28]. Nevertheless, here we use the structure (parton density) function method which systematically provides higher-order contributions enhanced by the large logarithms.

The article is organized as follows. In the next Section, ISR radiative corrections to electron-positron annihilation are discussed. In the third Section, we describe exponentiation procedures and suggest an expression for exponentiation of parton distribution function corresponding to both photonic and non-singlet pair corrections. The fourth Section is dedicated to the scheme dependence of the corrections. In the fifth Section, theoretical uncertainties are estimated and discussed.

2. ISR radiative corrections

Here we apply the parton distribution function (structure function) approach [4]. The cross section of electron-positron annihilation into a virtual photon or Z boson, decaying then, say, into muon pair

$$e^+e^- \to \gamma^*(Z^*) \to \mu^+\mu^- \tag{2}$$

with ISR corrections can be represented in the form of the convolution of two electron parton distribution functions (PDFs) and the partonic cross section [24]

$$\frac{d\sigma_{\bar{e}e}^{\mathrm{NNLL}}(s')}{ds'} = \sum_{i,j=e,\bar{e},\gamma} \int\limits_{\bar{z}_1}^{1} \int\limits_{\bar{z}_2}^{1} dz_1 dz_2 D_{ie}\left(z_1, \frac{\mu_R^2}{\mu_F^2}\right) D_{j\bar{e}}\left(z_2, \frac{\mu_R^2}{\mu_F^2}\right)$$
$$\times \left(\sigma_{ij}^{(0)}(sz_1z_2) + \overline{\sigma}_{ij}^{(1)}(sz_1z_2) + \overline{\sigma}_{ij}^{(2)}(sz_1z_2)\right)\delta(s' - sz_1z_2) + \mathscr{O}\left(\frac{m_e^2}{s}\right), \tag{3}$$

where $\bar{e} \equiv e^+$ is positron and $e \equiv e^-$ is electron, D_{ie} and $D_{j\bar{e}}$ are PDFs which define the probability density to find massless partons inside the massive electron (positron), $\sigma_{ij}^{(0,1,2)}$ are the Born (0), one-loop (1), and two-loop (2) contributions to cross-sections of annihilation into $\gamma^*(Z^*)$ at the partonic level, s is the initial center-of-mass energy squared, s' is the invariant mass of the produced virtual photon (or Z-boson) squared, and z is the energy fraction: $s' = sz$, $z \equiv z_1z_2$. Bars over $\overline{\sigma}_{ij}^{(1,2)}$ mean that these contributions are computed for massless partons within the $\overline{\mathrm{MS}}$ scheme for subtraction of electron mass singularities. For consistency, the PDFs are also defined in the $\overline{\mathrm{MS}}$ scheme.

The expansion of the master equation for cross-section takes into account the QED radiative corrections enhanced by the large logarithms and reads

$$\frac{d\sigma_{\bar{e}e}^{\mathrm{NNLL}}(s')}{ds'} = \frac{\sigma_{\bar{e}e}^{(0)}(s')}{s}\left\{\delta(1-z) + \sum_{\substack{k=1\\ k\geq l\geq k-2}}^{\infty} c_{kl}(z)\left(\frac{\alpha}{2\pi}\right)^k L^l + \mathscr{O}(\alpha^k L^{k-3})\right\}, \tag{4}$$

where $c_{kl}(z)$ are the coefficients to be computed. Here the sum can be divided into tree parts that consist of the leading (LL), next-to-leading (NLL), and next-to-next-to-leading (NNLL) logarithmic contributions ($l = k$, $l = k-1$, and $l = k-2$, respectively). Higher-order coefficients $c_{kl}(z)$ in the leading and next-to-leading logarithmic approximations up to c_{65} were first calculated in [29], and most of those coefficients were independently recalculated and corrected in [30]. Corrections to the results for c_{20} given in [24] can be found in [31] and [32].

To get the total cross section we have to integrate the differential cross section over z from

z_{min} corresponding to a certain minimal value of the invariant mass of the muon pair defined by experimental conditions,

$$\sigma_{e^+e^-} = \sigma^{(0)}(s) + \sum_{\substack{k=1\\ l\leq k}} \left(\frac{\alpha}{2\pi}\right)^k L^l \left[\int\limits_{z_{min}}^{1-\Delta} dz \sigma^{(0)}(sz) c^{\Theta}_{kl}(z) + c^{\Delta}_{kl}\sigma^{(0)}(s) \right]. \tag{5}$$

Here c^{Θ}_{kl} and c^{Δ}_{kl} are the so-called Θ and Δ parts of the coefficients c_{kl}, see details in [30]. The first corresponds to contributions from hard emission, and the second one corresponds to soft and virtual corrections. Δ is a small parameter dividing hard and soft contributions and is taken equal to 10^{-7} or 10^{-8}. The final result doesn't depend on Δ for $\Delta \to 0$. We present numerical results for relative corrections h_{kl} in percent separately in different orders in α and L:

$$h_{kl} = \left(\frac{\alpha}{2\pi}\right)^k L^l \left(\int\limits_{z_{min}}^{1-\Delta} dz \sigma^{(0)}(sz) c^{\Theta}_{kl}(z) + c^{\Delta}_{kl}\sigma^{(0)}(s) \right) / \sigma^{(0)}(s) \cdot 100\%. \tag{6}$$

We estimated numerical values of the leading and next-to-leading logarithmic corrections to initial state radiation in e^+e^--annihilation at different energies $\left(\frac{M_Z-1}{2}, \frac{M_Z}{2}, \frac{M_Z+1}{2}\right.$, 160 GeV, 240 GeV and 3 TeV$\left.\right)$ and different values of z_{min} (see Table A1). At 160 GeV and 240 GeV a radiative return to Z-resonance can occur due to the effective reduction of the collision energy because of radiation from the initial state, which makes the values of the corrections at $z_{min} = 0.1$ up to ten times larger than the same corrections at $\sqrt{s} = M_Z$. At $\sqrt{s} = 240$ GeV the return to the resonance is at $z \approx 0.14$, where $sz = M_Z^2$, and at $\sqrt{s} = 160$ GeV it is at $z \approx 0.32$.

We work within the collinear factorization framework, so we integrate over the angles of emitted photons. Note that the angular distribution of bremsstrahlung photons is peaked in the direction collinear to their parent charged particle momenta. In average, the angle of the emitted photons doesn't affect sufficiently inclusive observables such as the total cross section and the differential distribution in the invariant mass of the final-state fermion pair. For exclusive observables, one has to run a full Monte Carlo simulation and the collinear approximation can be used only as an estimate (adequately accurate Monte Carlo codes are not yet available).

3. Exponentiation

Exponentiation procedure allows resummation of a part of corrections that are most important in the domain of collinear and soft (or virtual) radiation. Exponentiation and resummation of QED corrections is discussed in details in [12].

Exponentiated pure photonic part of the electron PDF D_{ee} is given by the exact solution of the QED Dokshitzer-Gribov-Lipatov-Altarelli-Parisi (DGLAP) evolution equation found by V.N. Gribov and L.N. Lipatov in [11]:

$$D^{(exp,\gamma)}_{ee}(z;\beta) = \frac{\beta}{2} \frac{(1-z)^{\frac{\beta}{2}-1}}{\Gamma(\frac{\beta}{2}+1)} \exp\left(\frac{\beta}{2}\left(\frac{3}{4} - \gamma_E\right)\right), \tag{7}$$

for $\Theta-$part, where $\beta = \frac{2\alpha}{\pi}(L-1)$, Γ is the Euler Gamma-function, $\gamma_E \approx 0.577$ is the Euler-Mascheroni constant. We also need the $\Delta-$part for numerical applications:

$$D_{ee}^{(exp,\gamma)\Delta} \equiv \int\limits_{1-\Delta}^{1} dz D_{ee}^{(exp,\gamma)}(z;\beta) = \exp\left(\frac{\beta}{2}\ln\Delta + \frac{3\beta}{8}\right)\frac{\exp(-\gamma_E\beta/2)}{\Gamma(1+\beta/2)}. \quad (8)$$

As soon as the cross section has the structure $\sigma\otimes D\otimes D$, see Equation (3), we need to calculate the convolution of $D_{ee}^{(exp,\gamma)\otimes 2} = D_{ee}^{(exp,\gamma)}\otimes D_{ee}^{(exp,\gamma)}$ analytically. Technically it is very complicated, but we can present the $D_{ee}^{(exp,\gamma)\otimes 2}$ as

$$D_{ee}^{(exp,\gamma)\otimes 2}(z;\beta) \approx D_{ee}^{(exp,\gamma)}(z;2\beta). \quad (9)$$

This approximation becomes exact at $z\to 1$.

We suggest matching of the known perturbative higher-order corrections with the exponentiated result in the following form of an improved cross-section:

$$\sigma^{imp}(z) = \sigma^{pert}(z) - D_{ser}^{(exp,\gamma)\otimes 2}(z)\ \sigma^{(0)}(z) + D_{\infty}^{(exp,\gamma)\otimes 2}(z)\ \sigma^{(0)}(z), \quad (10)$$

where $D_{\infty}^{(exp,\gamma)\otimes 2}$ is the full exponentiated $D_{ee}^{(exp,\gamma)}\otimes D_{ee}^{(exp,\gamma)}$ given by Equation (9). Function $D_{ser}^{(exp,\gamma)\otimes 2}$ is obtained from $D_{\infty}^{(exp,\gamma)\otimes 2}$ by its expansion in series in α and L and keeping only contributions of those orders which are present in σ^{pert}, namely the leading and next-to-leading logarithmic contributions up to $\mathcal{O}(\alpha^5L^5)$ and $\mathcal{O}(\alpha^4L^3)$, respectively, together with $\mathcal{O}(\alpha^2L^0)$ terms. Let us remind that σ^{pert} is the result of our perturbative calculation [30]:

$$\sigma^{pert}(z) = D_{ee}\otimes D_{\bar{e}\bar{e}}\otimes\left(\sigma_{e\bar{e}}^{(0)}(z) + \frac{\alpha}{2\pi}\bar{\sigma}_{e\bar{e}}^{(1)}(z) + \left(\frac{\alpha}{2\pi}\right)^2\bar{\sigma}_{e\bar{e}}^{(2)}(z)\right)$$
$$+2D_{\gamma e}\otimes D_{\bar{e}\bar{e}}\otimes\left(\frac{\alpha}{2\pi}\sigma_{e\gamma}^{(0)}(z) + \left(\frac{\alpha}{2\pi}\right)^2\bar{\sigma}_{e\gamma}^{(1)}(z)\right) + D_{\bar{e}e}\otimes D_{e\bar{e}}\otimes\left(\frac{\alpha}{2\pi}\sigma_{e\bar{e}}^{(0)}(z) + \left(\frac{\alpha}{2\pi}\right)^2\bar{\sigma}_{e\bar{e}}^{(1)}(z)\right). \quad (11)$$

Here D_{ab} are structure functions obtained by iterative solution of the DGLAP equation. In this way, we perform matching of the perturbative results with the exponentiated ones and avoid double counting. Despite the fact that we have explicit perturbative results only in the LL and NLL approximations and the one $\mathcal{O}(\alpha^2L^0)$ next-to-next-to-leading correction (h_{20}), we take into account in $D_{ser}^{(exp,\gamma)\otimes 2}$ all terms up to $\mathcal{O}(\alpha^5L^0)$ appearing in the expansion. All these higher-order corrections are present in $D_{\infty}^{(exp,\gamma)\otimes 2}$, and then cancel each other when we calculate an improved cross section according to Equation (10). Note that in $D_{ser}^{(exp,\gamma)\otimes 2}(z)\ \sigma^{(0)}(z)$ and $D_{\infty}^{(exp)\otimes 2}(z)\ \sigma^{(0)}(z)$ there is no $\bar{\sigma}^{(1)}$ because all soft and virtual contributions are included into $D^{(exp)\otimes 2}$ and because the exponentiated expressions are applicable at $z\to 1$ but $\bar{\sigma}^{(1)}$ tends to zero in this area. To obtain numerical value of the improved cross-section we have to integrate it from some z_{min}, defined by experimental conditions, to 1.

We can estimate the h_{55} pure photonic correction the following way:

$$h_{55,\gamma}^{exp} = \left(\int\limits_{z_{min}}^{1} dz D_{ser,55}^{(exp,\gamma)\otimes 2}(z)\ \sigma^{(0)}(sz)\right)/\sigma^{(0)}(s)\cdot 100\%, \quad (12)$$

where $D_{ser,55}^{(exp,\gamma)\otimes 2}(z)$ is the part of the expansion that consists of only $\mathcal{O}(\alpha^5L^5)$ terms. The values of $h_{55,\gamma}^{exp}$ are presented in percent with respect to Born cross section. Numerical values of the full pure photonic h_{55}

and approximated $h^{exp}_{55,\gamma}$ corrections are close to each other, as can be seen from Table A1, which justifies application of the exponentiation for estimates of further higher-order contributions.

We can also estimate the residual "tail" consisting of higher-order contributions provided by the exponentiated result beyond the perturbative one:

$$\Delta^{DD\sigma}_{\infty,\gamma} = \left(\int\limits_{z_{min}}^{1} dz D^{(exp,\gamma)\otimes 2}_{\infty}(z)\ \sigma^{(0)}(sz) - \int\limits_{z_{min}}^{1} dz D^{(exp,\gamma)\otimes 2}_{ser}(z)\ \sigma^{(0)}(sz) \right) / \sigma^{(0)}(s) \cdot 100\%. \tag{13}$$

We can also estimate pair corrections. Only non-singlet (NS) pair corrections can be exponentiated since the singlet ones are not enhanced at $z \to 1$. Pair contributions come from the running α and the splitting functions. The space-like NLO splitting function of the electron in electron type can be divided into four parts corresponding to pure photonic (γ) contributions, non-singlet pair (NS) ones, singlet pair (S) ones, and the interference (int) of the latter two ones:

$$P^{(1)\gamma}_{ee} = 2\left(\frac{1+x^2}{1-x}\left[-\ln x \ln(1-x) + \frac{1}{2}\ln^2 x + \mathrm{Li}_2(1-x)\right] + \ln x + \frac{3}{2} - x + \frac{1}{4}(1+x)\ln^2 x\right), \tag{14}$$

$$P^{(1)NS}_{ee} = 2\left(-\frac{1}{3}\frac{1+x^2}{1-x} - \frac{2}{3}(1-x)\right), \tag{15}$$

$$P^{(1)S}_{ee} = \frac{20}{9x} - 2 + 6x - \frac{56}{9}x^2 + (1 + 5x + \frac{8}{3}x^2)\ln x - (1+x)\ln^2 x, \tag{16}$$

$$P^{(1)int}_{ee} = 2\left(\frac{1+x^2}{1+x}\left(-\frac{1}{2}\ln^2 x \mathrm{Li}_2(1-x) - \frac{3}{4}\ln x\right) - \frac{7}{4}(1+x)\ln x - 4 + \frac{7}{2}x\right). \tag{17}$$

In the work [33] exponentiation of QCD corrections for Drell-Yan and deep inelastic scattering (DIS) processes was discussed taking into account pair corrections. An exponentiation of non-singlet pair and photonic corrections can also be constructed as a sum of two "exponents". Here we suggest to perform a joint exponentiation of pure photonic and non-singlet pair corrections in electron PDF. We use the same structure as the expression for pure photonic corrections but modify the parameter β as follows:

$$\begin{aligned} D^{(exp,\gamma+NS)}_{ee}(z;\tilde{\beta}) &= \frac{\tilde{\beta}}{2}(1-z)^{\frac{\tilde{\beta}}{2}-1}\exp\left(\frac{3}{4}\frac{\tilde{\beta}}{2}\right)\frac{\exp(-\gamma_E\tilde{\beta}/2)}{\Gamma(1+\tilde{\beta}/2)}, \\ \tilde{\beta} &\equiv \frac{2\alpha}{\pi}(L-1)\left(1+\frac{\alpha}{6\pi}\left(L-\frac{7}{3}\right)\right). \end{aligned} \tag{18}$$

The number $\frac{7}{3}$ was obtained from the comparison of the expanded exponent with the perturbative expression. This coefficient was adjusted to make the terms proportional to $1/(1-z)$ in the contribution of the order $\alpha^2 L^1$ being equal. The Δ-part of this expression is constructed analogously to Equation (8):

$$D^{(exp,\gamma+NS)\Delta}_{ee} = \exp\left(\frac{\tilde{\beta}}{2}\ln\Delta + \frac{3\tilde{\beta}}{8}\right)\frac{\exp(-\gamma_E\tilde{\beta}/2)}{\Gamma(1+\tilde{\beta}/2)}. \tag{19}$$

Note that Equation (18) takes into account pure photonic contributions, pure non-singlet pair ones, and mixed (photonic + non-singlet pair) corrections. We can estimate photonic plus non-singlet pair corrections in the same way as in Equation (12), and $\Delta^{DD\sigma}_{\infty,\gamma+NS}$ the same way as in Equation (13). In

Table A1, they are presented in the columns h_{55}^{exp} and $\Delta_{\infty}^{DD\sigma}$ correspondingly, pure photonic case is shown in the rows marked "γ", and photonic plus non-singlet pair case is shown in the rows marked "Full". In Figure 1 we show the dependence of the contribution of the exponentiation "tail" $\Delta_{\infty,\gamma+NS}^{DD\sigma}$ on the center-of-mass energy for three different values of the cut value z_{min}. One can see that the effect of exponentiation is can be relevant numerically if the precision level of 10^{-4} in the total cross section measurement will be achieved. The relatively wide deep in the case of $z_{min}=0.1$ corresponds to the effect of the radiative return to the Z resonance.

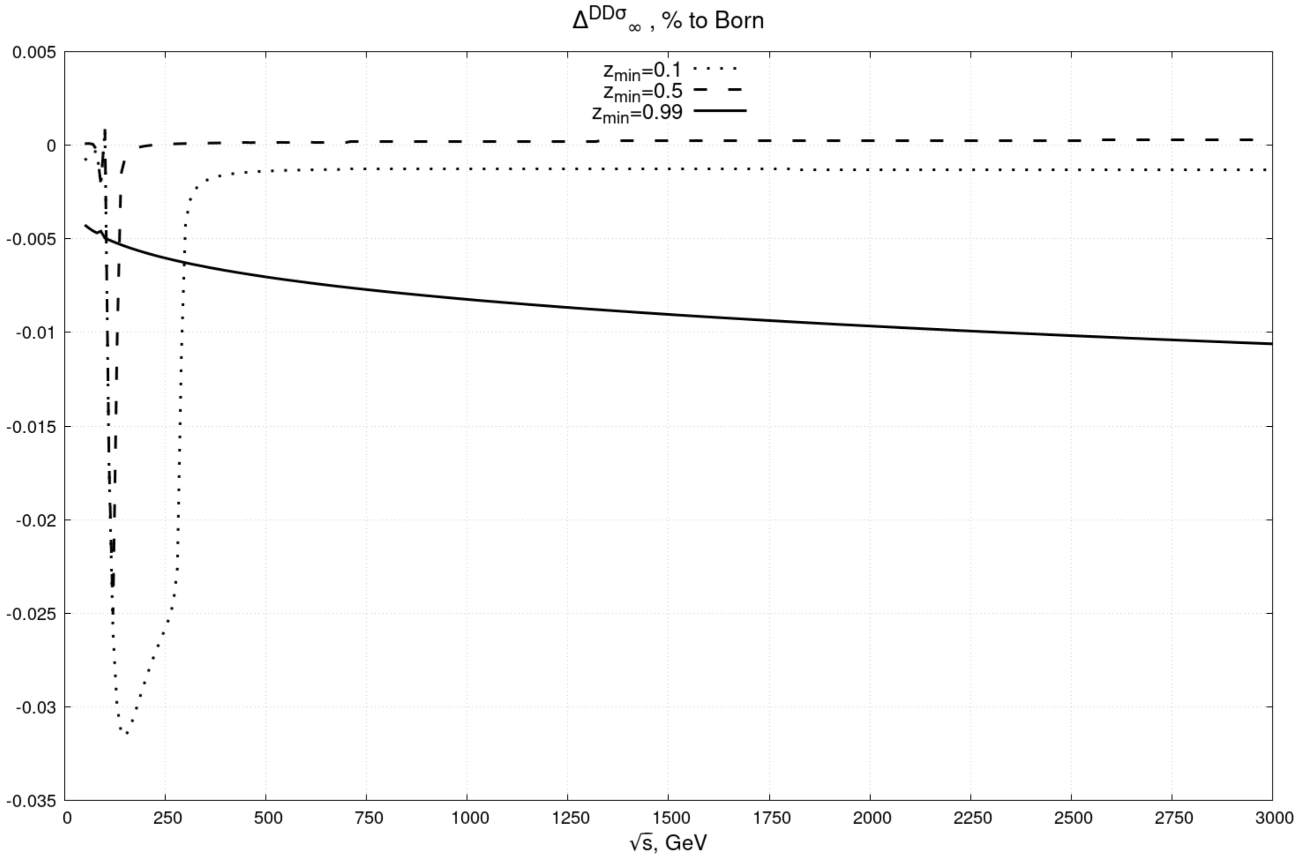

Figure 1. $\Delta_{\infty,\gamma+NS}^{DD\sigma}$ in percent *vs.* center-of-mass energy for three different values of z_{min}.

4. Scheme dependence

Despite the fact that the sum of all corrections of particular order in α doesn't depend neither on the factorization scale value nor on the subtraction scheme choice, the expressions for individual contributions are scheme-dependent. In the $\overline{\text{MS}}$ scheme we use the following initial conditions for the evolution equation:

$$d_{ee}^{(1)}(x) = \left[\frac{1+x^2}{1-x}(-1-2\ln(1-x))\right]_+, \tag{20}$$

$$d_{\gamma e}^{(1)}(x) = -\frac{1+(1-x)^2}{x}(2\ln x+1), \tag{21}$$

$$d_{e\gamma}^{(1)}(x) = 0, \tag{22}$$

and the expression for the relevant NLO splitting function reads

$$P_{ee}^{(1)\Theta}(x) = -\frac{56x^2}{9} + \left(\frac{8x^2}{3} + \frac{11x}{3} - \frac{13}{3(1-x)} + \frac{5}{3}\right)\ln(x) + \frac{37x}{3} + \frac{20}{9x} - \left(\frac{3x}{2} + \frac{3}{2}\right)\ln^2(x)$$
$$+ \left((2x+2)\ln(1-x) - \frac{4\ln(1-x)}{1-x}\right)\ln(x) - \frac{25}{3},$$
$$P_{ee}^{(1)\Delta} = \frac{15}{8} - \frac{13}{3}\zeta_2 + 6\zeta_3. \tag{23}$$

In Equation (20) the subscript "+" means the standard plus prescription. If we compare an expression for $D_{ee}(x)$ obtained from iterative solution of the evolution equation in the $\overline{\mathrm{MS}}$ scheme with the $D_{ser}^{(exp,\gamma)}$, we can see that the $\overline{\mathrm{MS}}$ scheme generates higher powers of $\ln(1-z)$ than exponentiation due to the presence of $\frac{1+x^2}{1-x}\ln(1-x)$ in $d_{ee}^{(1)}$. In order-by-order calculations those singular at $z \to 1$ extra terms (they do not correspond to any soft or collinear singularities) cancel out with the corresponding terms from convolution of the leading-order structure function with the next-to-leading order partonic cross section $\overline{\sigma}^{(1)}$. But in the exponentiated $D^{(exp\otimes 2)}$ multiplied by $\sigma^{(0)}$ they don't cancel out.

We suggest another factorization scheme, where

$$\tilde{d}_{ee}^{(1)}(x) = -\left[\frac{1+x^2}{1-x}\right]_+. \tag{24}$$

So, we change $d_{ee}^{(1)}$ and derive the corresponding expressions for $\widetilde{\sigma}^{(1)}$ and $P_{ee}^{(1)}$ from matching equalities at $\mathcal{O}(\alpha^1)$ [30] and $\mathcal{O}(\alpha^2)$:

$$\delta_{\bar{e}e}^{(1)}(sx) = \bar{\delta}_{\bar{e}e}^{(1)}(sx) + 2\frac{\alpha}{2\pi}\left[P_{ee}^{(0)}(y)L + d_{ee}^{(1)}(y)\right] + \mathcal{O}\left(\frac{m_e^2}{s}\right), \tag{25}$$

where $\bar{\delta}_{\bar{e}e}^{(1)}(sx) \equiv \frac{\overline{\sigma}_{\bar{e}e}^{(1)}(sx)}{\sigma_{\bar{e}e}^{(0)}(sx)}$ and $\delta_{\bar{e}e}^{(1)}(sx) \equiv \frac{\sigma_{\bar{e}e}^{(1)}(sx)}{\sigma_{\bar{e}e}^{(0)}(sx)}$, and

$$\delta_{\bar{e}e}^{(2)}(sx) = \left(\frac{\alpha}{2\pi}\right)^2 L^2\left[P_{e\gamma}^{(0)} \otimes P_{\gamma e}^{(0)} + \frac{2}{3}P_{ee}^{(0)} + 2P_{ee}^{(0)\otimes 2}\right] + \left(\frac{\alpha}{2\pi}\right)^2 L\left[2\bar{\delta}_{e\gamma}^{(0)} \otimes P_{\gamma e}^{(0)} + \frac{2}{3}\bar{\delta}_{\bar{e}e}^{(1)}\right.$$
$$\left. + 2\bar{\delta}_{\bar{e}e}^{(1)} \otimes P_{ee}^{(0)} + 2d_{\gamma e}^{(1)} \otimes P_{e\gamma}^{(0)} + 2P_{ee}^{(1)} - \frac{20}{9}P_{ee}^{(0)} + 4P_{ee}^{(0)} \otimes d_{ee}^{(1)}\right] + \left(\frac{\alpha}{2\pi}\right)^2 c_{20}. \tag{26}$$

We omit the arguments on the right-hand side for brevity. Functions $\overline{\sigma}^{(2)}$ and $d_{ee}^{(2)}$, which will appear in c_{20}, must change due to change of $d_{ee}^{(1)}$, $P_{ee}^{(1)}$ and $\overline{\sigma}^{(1)}$. We assume that $P_{e\gamma}^{(1)}$, $P_{\gamma e}^{(1)}$, and $d_{\gamma e}^{(0)}$ don't change because they contain no unphysical logarithms. From this we can conclude that it is enough to consider the sum

$$\frac{2}{3}\bar{\delta}_{\bar{e}e}^{(1)} + 2\bar{\delta}_{\bar{e}e}^{(1)} \otimes P_{ee}^{(0)} + 2P_{ee}^{(1)} + 4P_{ee}^{(0)} \otimes d_{ee}^{(1)}, \tag{27}$$

which must not change for matching. In our new scheme, we have

$$\widetilde{P}_{ee}^{(1)}(x) = P_{ee}^{(1)}(x) + \frac{4}{3}(1+x^2)\frac{\ln(1-x)}{1-x},$$
$$\widetilde{P}_{ee}^{(1)\Delta} = -\frac{11}{12} + \frac{8}{3}\ln^2\Delta - \frac{26}{3}\zeta_2,$$
$$\widetilde{\overline{\sigma}}_{ee}^{(1)}(x) = 2\frac{1+x^2}{1-x}(\ln z - \ln x), \tag{28}$$
$$\widetilde{\overline{\sigma}}_{ee}^{(1)\Delta} = 4\zeta_2 - 1. \tag{29}$$

In our new scheme $\widetilde{\overline{\sigma}}^{(1)}_{ee}$ has its theta part equal to zero at $x = z$, and convolutions become significantly easier.

5. Theoretical uncertainty

We can estimate the following three different contributions to theoretical uncertainty:

$$\Delta_{LL,exp} = \frac{h_{55}}{h_{44}}(h_{55}^{(exp)} - h_{55}), \tag{30}$$

$$\Delta_{NLL} = \frac{h_{43}}{h_{32}} h_{43}, \tag{31}$$

$$\Delta_{NNLL} = \frac{h_{20}}{h_{21}} h_{32}. \tag{32}$$

Equation (30) estimates the uncertainty in h_{66}; Equation (31) estimates the unaccounted NLL contribution h_{54}, and Equation (32) estimates the unaccounted NNLL contribution h_{31}. In the Table 1 we present the results for calculating uncertainties at the Z-peak where the highest experimental precision of the order of $10^{-3}\%$ can be achieved at future colliders in the so-called Tera-Z mode [34].

Table 1. Theoretical uncertainty in % at $\sqrt{s} = M_Z$.

z_{min}	$\Delta_{LL,exp}$	Δ_{NLL}	Δ_{NNLL}
0.1	0.00019	0.00014	0.00036
0.5	0.00019	0.00014	0.00036
0.9	0.00021	0.00014	0.00035

Here all the values are in percent with respect to Born cross section, so the current theoretical uncertainty in description of ISR in the total cross section at Z-peak can be estimated to be about $4 \cdot 10^{-4}\%$. Obviously, calculation of the h_{31} contribution should be the next step to improve the accuracy.

At the energy $\sqrt{s} = 240$ GeV the uncertainty is bigger for $z_{min} = 0.1$ because of the radiative return to the resonance, but the experimental requirements are not so strict. Uncertainties in this energy domain will be considered elsewhere.

6. Conclusion

So, we constructed matching of the existing perturbative results for the leading and next-to-leading higher-order ISR corrections to processes of e^+e^--annihilation with simultaneous exponentiation of certain photonic and pair corrections. The matching allows one to combine the advantages of the two approaches and thus to improve the resulting precision. Note that any future perturbative result can be easily incorporated within the proposed scheme.

Numerical values of LL and NLL ISR corrections to the cross section of electron-positron annihilation in $\overline{\text{MS}}$ scheme were calculated. The calculations will be implemented in the ZFITTER program [35]. The suggested new subtraction scheme is useful for evaluation of radiative corrections within the QED structure approach, especially for $z \to 1$. The theoretical uncertainty in the description of radiative corrections in e^+e^- annihilation processes should still be improved by inclusion of new perturbative calculations, including effects due to the final state radiation (FSR) and ISR-FSR interference.

The presented numerical results are obtained for inclusive treatment of the ISR effects. Alternatively, one can apply QED parton showers, which are a kind of exponentiated description of ISR in a differential form. If the latter is relevant for a given observable, one should perform matching of the completely differential perturbative results with parton showers. Our work on this task is in progress within the ReneSANCe Monte Carlo event generator [36].

Data availability statement

No supplementary or additional data were generated in this study.

Declaration of generative AI and AI-assisted technologies

The authors did not use generative AI or AI-assisted technologies in the writing of this manuscript.

Acknowledgments

We are grateful to A.V. Kotikov for fruitful discussions.

Authors' contribution

Conceptualization, A.A. and U.V.; methodology, A.A. and U.V.; software, A.A. and U.V.; validation, A.A. and U.V.; formal analysis, A.A. and U.V.; investigation, A.A. and U.V.; data curation, A.A. and U.V.; writing—original draft preparation, A.A. and U.V.; writing—review and editing, A.A. and U.V.; supervision, A.A.; project administration, A.A. All authors have read and agreed to the published version of the manuscript.

Conflicts of interest

Andrej Arbuzov holds the position of Advisory Board Member for *Asymmetry* and has not peer reviewed or made any editorial decisions for this paper. The authors declare no conflicts of interest.

Appendix

Here we present Table A1 with numerical results for particular contributions.

Table A1. Numerical values of radiative corrections, %.

	h_{11}	h_{10}	h_{22}	h_{21}	h_{20}	h_{33}	h_{32}	h_{44}	h_{43}	h_{55}	h_{55}^{exp}	$\Delta_{\infty}^{DD\sigma}$
$\sqrt{s}=M_Z-1$												
$z_{min}=0.1$												
γ	−37.62744	2.20532	7.28672	−0.82576	0.02063	−0.95300	0.15752	0.09393	−0.02019	−0.00737	−0.00714	−0.00200
Pairs	0	0	−0.35072	0.20364	−0.03280	0.13186	−0.08364	−0.02446	0.01642	0.00297	-	-
Full	−37.62744	2.20532	6.93600	−0.62292	−0.01217	−0.82114	0.07388	0.06947	−0.00377	−0.00441	−0.00385	−0.00216
$z_{min}=0.5$												
γ	−37.66044	2.2067	7.28480	−0.82656	0.02065	−0.95285	0.15746	0.09393	−0.02019	−0.00737	−0.00715	−0.00200
Pairs	0	0	−0.35204	0.2038	−0.03277	0.13185	−0.08363	−0.002446	0.01642	0.00297	-	-
Full	−37.66044	2.2067	6.93272	−0.62276	−0.01213	−0.82101	0.07383	0.06947	−0.00377	−0.00440	−0.00386	−0.00216
$z_{min}=0.9$												
γ	−38.07502	2.22386	7.2852	−0.82684	0.02085	−0.95183	0.15758	0.09337	−0.02007	−0.00732	−0.00706	−0.00202
Pairs	0	0	−0.35244	0.20392	−0.03288	0.13271	−0.08393	−0.02442	0.01637	0.00295	-	-
Full	−38.07502	2.22386	6.93272	−0.62276	−0.01203	−0.81912	0.07365	0.06895	−0.00370	−0.00438	−0.00382	−0.00216
$z_{min}=0.99$												
γ	−46.70978	2.59612	10.41804	−1.14888	−0.02851	−1.40697	0.23324	0.12309	−0.02747	−0.00622	− 0.00597	−0.00462
Pairs	0	0	−0.44028	0.2706	−0.04487	0.18941	−0.12097	−0.03622	0.02306	0.00380	-	-
Full	−46.70978	2.59612	9.9778	−0.87832	−0.01636	−1.21756	0.11228	0.008687	−0.00441	−0.00242	−0.00169	−0.00462
$\sqrt{s}=M_Z+1$												
$z_{min}=0.1$												
γ	−10.85409	1.09644	−3.20789	0.21972	−0.00441	1.04577	−0.15565	−0.14951	0.03139	0.01349	0.01371	0.00090
Pairs	0	0	−0.10032	−0.00757	0.01180	−0.06152	0.06022	0.02836	−0.02194	−0.00498	-	-
Full	−10.85409	1.09644	−3.30821	0.21215	0.00738	0.98425	−0.09543	−0.12115	0.00945	0.00850	0.00832	0.00238
$z_{min}=0.5$												
γ	−10.88572	1.09775	−3.20974	0.21972	−0.00440	1.04590	−0.15571	−0.14950	0.03139	0.01349	0.01370	0.00090
Pairs	0	0	−0.10159	−0.00742	0.01182	−0.06153	0.06023	0.02836	−0.02194	−0.00498	-	-
Full	−10.88572	1.09775	−3.31133	0.21230	0.00742	0.98438	−0.09548	−0.12114	0.00945	0.00850	0.00832	0.00238
$z_{min}=0.9$												
γ	−11.55686	1.12548	−3.12720	0.20817	−0.00407	1.04707	−0.15539	−0.15045	0.03158	0.01357	0.01381	0.00087
Pairs	0	0	−0.10808	−0.00438	0.01163	−0.06003	0.05969	0.02842	−0.02203	−0.00502	-	-
Full	−11.55686	1.12548	−3.23528	0.20379	0.00756	0.98704	−0.09571	−0.12206	0.00905	0.00855	0.00838	0.00238
$z_{min}=0.99$												
γ	−39.28805	2.27114	6.15316	−0.74405	0.01908	−0.26952	0.06537	−0.07252	0.01158	0.01794	0.01828	−0.00705
Pairs	0	0	−0.36817	0.19250	−0.02386	0.11072	−0.04958	−0.00566	−0.00330	−0.00285	-	-
Full	−39.28805	2.27114	5.78498	−0.55155	−0.00477	−0.15880	0.01579	−0.07818	0.00828	0.01509	0.01551	−0.00493
$\sqrt{s}=M_Z$												
$z_{min}=0.1$												
γ	−32.73654	2.00167	4.88428	−0.59516	0.01521	−0.37760	0.07104	0.00344	−0.00185	0.00315	0.00341	-0.00270
Pairs	0	0	−0.30571	0.15847	−0.02152	0.08758	−0.04604	−0.00909	0.00375	−0.00008	-	-
Full	−32.73654	2.00167	4.57858	−0.43669	−0.00631	−0.29002	0.02500	−0.00564	0.00190	0.00307	0.00344	−0.00194
$z_{min}=0.5$												
γ	−32.75622	2.00249	4.88313	−0.59516	0.01521	−0.37751	0.07101	0.00345	−0.00185	0.00315	0.00341	−0.00270
Pairs	0	0	−0.30650	0.15857	−0.02150	0.08757	−0.04603	0.00908	0.00375	−0.00008	-	-
Full	−32.75622	2.00249	4.57663	−0.43660	−0.00629	−0.28994	0.02497	−0.00564	0.00190	0.00307	0.00344	−0.00194
$z_{min}=0.9$												
γ	−33.0710	2.01547	4.92033	−0.60045	0.01537	−0.37684	0.07112	0.00301	−0.00176	0.00319	0.00345	−0.00271
Pairs	0	0	−0.30954	0.15997	−0.02157	0.08824	−0.04627	0.00905	0.00371	−0.00009	-	-
Full	−33.0710	2.01547	4.61079	−0.44048	−0.00622	−0.28860	0.02485	−0.00604	0.00195	0.00310	0.00347	−0.00194

Table A1. *Cont.*

	h_{11}	h_{10}	h_{22}	h_{21}	h_{20}	h_{33}	h_{32}	h_{44}	h_{43}	h_{55}	h_{55}^{exp}	$\Delta_{\infty}^{DD\sigma}$
$\sqrt{s} = 160$ GeV												
$z_{min} = 0.1$												
γ	335.79956	−12.62015	17.14787	0.64666	−0.11553	−1.82233	0.57813	−0.03476	−0.01018	0.00562	0.01695	−0.03213
Pairs	0	0	8.35391	−1.84375	−0.14402	0.13309	−0.09339	−0.06055	0.03570	−0.00164	-	-
Full	335.79956	−12.62015	25.50178	−1.19709	−0.25954	−1.68924	0.48483	−0.09531	0.02552	0.00397	0.02057	−0.00312
$z_{min} = 0.5$												
γ	9.81624	0.26017	−1.28618	0.20722	−0.00761	−0.00845	−0.00714	0.00530	−0.00153	−0.00022	−0.00097	0.00032
Pairs	0	0	0.13182	−0.05573	−0.00427	−0.02757	0.01162	−0.00171	0.00046	0.00020	-	-
Full	9.81624	0.26017	−1.15435	0.15149	−0.01188	−0.03602	0.00447	0.00359	−0.00107	0.00002	−0.00018	−0.00039
$z_{min} = 0.9$												
γ	−17.49251	1.33920	0.37598	−0.11629	0.00320	0.17976	−0.02564	−0.02424	0.00549	0.00143	0.00156	0.00072
Pairs	0	0	−0.17090	0.05814	−0.00496	0.00499	0.00377	0.00511	−0.00376	−0.00083	-	-
Full	−17.49251	1.33920	0.20508	−0.05815	−0.00177	0.18475	−0.02187	−0.01912	0.00174	0.00058	0.00060	0.000103
$\sqrt{s} = 240$ GeV												
$z_{min} = 0.1$												
γ	324.14638	−11.76206	27.12979	−0.99088	−0.08026	−0.62423	0.61404	−0.06641	0.01487	0.00247	0.02316	−0.03299
Pairs	0	0	25.33367	−1.47717	−0.44478	−0.02167	−0.03074	−0.01918	0.04599	0.00012	-	-
Full	324.14638	−11.76206	52.46346	−2.46805	−0.52504	−0.63690	0.58330	−0.08559	0.06086	0.00259	0.01950	−0.02631
$z_{min} = 0.5$												
γ	3.45872	0.51562	−1.05495	0.14324	−0.00510	0.02506	−0.01176	0.00273	−0.00067	−0.00020	−0.00089	0.00059
Pairs	0	0	0.05956	−0.02900	−0.00412	−0.02361	−0.01040	0.00046	−0.00017	0.00013	-	-
Full	3.45872	0.51562	−0.99539	0,11424	−0.00923	0,00145	−0,00136	0.00319	−0,00084	−0,00007	−0.00005	0.00003
$z_{min} = 0.9$												
γ	−18.60745	1.36043	0.56697	−0.13653	0.00358	0.17533	−0.02372	−0.02589	0.00568	0.00161	0.00179	0.00063
Pairs	0	0	−0.18765	0.06353	−0.00549	0.00878	0.00216	0.00551	−0.00380	−0.00092	-	-
Full	−18.60745	1.36043	0.37931	−0.07300	−0.00191	0.18411	−0.02157	−0.02038	0.00188	0.00069	0.00073	0.00098
$\sqrt{s} = 3$ TeV												
$z_{min} = 0.1$												
γ	19.53776	0.02118	0.03886	0.14215	−0.00856	−0.06571	0.02188	0.00028	−0.00096	0.0001	0.00014	−0.00066
Pairs	0	0	1.03833	−0.11012	−0.01629	−0.02899	0.00887	−0.00263	0.00276	−0.01574	-	
Full	19.53776	0.02118	1.07719	0.03203	−0.02485	−0.0947	0.03075	0.00235	0.00180	−0.01564	0.00148	−0.00133
$z_{min} = 0.5$												
γ	2.22920	0.57652	−1.34517	0.14759	−0.00447	0.04977	−0.01709	0.00413	−0.00078	−0.00043	−0.00195	0.00113
Pairs	0	0	0.05826	−0.02631	−0.00422	−0.03629	0.01365	0.00126	−0.00047	0.00024	-	-
Full	2.22920	0.57652	−1.28691	0.12128	−0.00869	0.01349	−0.00344	0.00539	−0.00125	−0.00018	−0.00073	0.00027
$z_{min} = 0.9$												
γ	−22.44302	1.36803	0.89303	−0.17003	0.00371	0.28417	−0.03192	−0.05129	0.00942	0.00384	0.00428	0.00052
Pairs	0	0	−0.27012	0.07734	−0.00568	0.01695	0.00211	0.01072	−0.00624	−0.00218	-	-
Full	−22.44302	1.36803	0.06229	−0.0927	−0.00197	0.30112	−0.02981	−0.04056	0.00318	0.00166	0.00179	0.00114

References

[1] Abada A, Abbrescia M, AbdusSalam SS, Abdyukhanov I, Abelleira Fernandez J, *et al.* FCC-ee: the lepton collider: future circular collider conceptual design report volume 2. *Eur. Phys. J. Spec. Top.* 2019, 228(2):261–623.

[2] The CEPC Study Group. CEPC conceptual design report: volume 2—physics & detector. *arXiv* 2018, arXiv:1811.10545.

[3] The FCC Collaboration. FCC physics opportunities: future circular collider conceptual design report volume 1. *Eur. Phys. J. C* 2019, 79(6):474.

[4] Kuraev EA, Fadin VS. On radiative corrections to e^+e^- single photon annihilation at high-energy. *Sov. J. Nucl. Phys.* 1985, 41:466–472.

[5] Yennie DR, Frautschi SC, Suura H. The infrared divergence phenomena and high-energy processes. *Annals Phys.* 1961, 13:379–452.

[6] Golonka P, Was Z. PHOTOS Monte Carlo: a precision tool for QED corrections in Z and W decays. *Eur. Phys. J. C* 2006, 45(1):97–107.

[7] Jadach S, Ward B, Was Z. The precision Monte Carlo event generator KK for two-fermion final states in e^+e^- collisions. *Comput. Phys. Commun.* 2000, 130(3):260–325.

[8] Jadach S, Richter-Was E, Ward BFL, Was Z. Monte Carlo program BHLUMI-2.01 for Bhabha scattering at low angles with Yennie-Frautschi-Suura exponentiation. *Comput. Phys. Commun.* 1992, 70:305–344.

[9] Płaczek W, Skrzypek M, Ward BFL, Yost SA. Bhabha scattering at future colliders with BHLUMI/BHWIDE. *arXiv* 2026, arXiv:2601.15265.

[10] Krauss F, Price A, Schonherr M. YFS resummation for future lepton-lepton colliders in SHERPA. *SciPost Phys.* 2022, 13(2):026.

[11] Gribov VN, Lipatov LN. e^+e^- pair annihilation and deep inelastic ep scattering in perturbation theory. *Sov. J. Nucl. Phys.* 1972, 15:675–684.

[12] Passarino G. A Practical approach for exponentiation of QED corrections in arbitrary processes. *Nucl. Phys. B* 2001, 619:313–358.

[13] Ward BFL, Jadach S, Placzek W, Skrzypek M, Was Z, *et al.* Recent developments in IR-improved amplitude-based resummation in precision high energy collider physics. *arXiv* 2026, arXiv:2604.26124.

[14] Jadach S, Ward BFL, Was Z. Coherent exclusive exponentiation CEEX: the case of the resonant e^+e^- collision. *Phys. Lett. B* 1999, 449:97–108.

[15] Jadach S, Ward BFL. Exclusive exponentiation in the Monte Carlo Yennie-Frautschi-Suura approach. In *NATO ASI Series*, 1st ed. New York: Springer, 1989. pp. 325–340.

[16] Frixione S, Laenen E, Carloni Calame C, Denner A, Dittmaier S, *et al.* Initial state QED radiation aspects for future e^+e^- colliders. *arXiv* 2022, arXiv:2203.12557.

[17] Gribov VN, Lipatov LN. Deep inelastic ep scattering in perturbation theory. *Sov. J. Nucl. Phys.* 1972, 15:438–450.

[18] Altarelli G, Parisi G. Asymptotic freedom in parton language. *Nucl. Phys. B* 1977, 126:298–318.

[19] Dokshitzer YL. Calculation of the structure functions for deep inelastic scattering and e^+e^- annihilation by perturbation theory in quantum chromodynamics. *Sov. Phys. JETP* 1977, 46:641–653.

[20] Nicrosini O, Trentadue L. Soft photons and second order radiative corrections to e^+e^- —> Z0. *Phys. Lett. B* 1987, 196:551.

[21] Skrzypek M. Leading logarithmic calculations of QED corrections at LEP. *Acta Phys. Polon. B* 1992, 23:135–172.

[22] Cacciari M, Deandrea A, Montagna G, Nicrosini O. QED structure functions: a systematic approach. *EPL* 1992, 17:123–128.

[23] Actis S, Arbuzov A, Balossini G, Beltrame P, Bignamini C, *et al.* Quest for precision in hadronic cross sections at low energy: Monte Carlo tools *vs.* experimental data. *Eur. Phys. J. C* 2010, 66:585–686.

[24] Berends FA, Van Neerven WL, Burgers GJH. Higher order radiative corrections at LEP energies. *Nucl. Phys. B* 1988, 297:429–478.

[25] Blumlein J, Kawamura H. $O(\alpha^2 L)$ radiative corrections to deep inelastic ep scattering. *Phys. Lett. B* 2003, 553:242–250.

[26] Tomalak O, Chen Q, Hill RJ, McFarland KS. QED radiative corrections for accelerator neutrinos. *Nature Commun.* 2022, 13(1):5286.

[27] Tomalak O, Chen Q, Hill RJ, McFarland KS, Wret C. Theory of QED radiative corrections to neutrino scattering at accelerator energies. *Phys. Rev. D* 2022, 106(9):093006.

[28] Hill RJ. Effective field theory for large logarithms in radiative corrections to electron proton scattering. *Phys. Rev. D* 2017, 95(1):013001.

[29] Ablinger J, Blumlein J, De Freitas A, Schonwald K. Subleading logarithmic QED initial state corrections to $e^+e^- \to \gamma^*/Z_0^*$ to $O(\alpha^6 L^5)$. *Nucl. Phys. B* 2020, 955:115045.

[30] Arbuzov A, Voznaya U. Higher-order NLO initial state QED radiative corrections to e^+e^- annihilation revisited. *Phys. Rev. D* 2024, 109(11):113002.

[31] Blumlein J, De Freitas A, Raab CG, Schonwald K. The $O(\alpha^2)$ initial state QED corrections to e^+e^- annihilation to a neutral vector boson revisited. *Phys. Lett. B* 2019, 791:206–209.

[32] Hamberg R, van Neerven WL, Matsuura T. A complete calculation of the order $\alpha - s^2$ correction to the Drell-Yan K factor. *Nucl. Phys. B* 1991, 359:343–405.

[33] Catani S, Trentadue L. Resummation of the QCD perturbative series for hard processes. *Nucl. Phys. B* 1989, 327:323–352.

[34] Blondel A, Gluza J, Jadach S, Janot P, Riemann T, *et al.* Standard model theory for the FCC-ee Tera-Z stage. *arXiv* 2018, arXiv:1809.01830.

[35] Akhundov A, Arbuzov A, Riemann S, Riemann T. The ZFITTER project. *Phys. Part. Nucl.* 2014, 45(3):529–549.

[36] Sadykov R, Yermolchyk V. Polarized NLO EW e^+e^- cross section calculations with ReneSANCe-v1.0.0. *Comput. Phys. Commun.* 2020, 256:107445.